Using Radar Chart Areas to Evaluate the Sensitivity of Electronic Nose Sensors in Detecting Water Stress in Soybean

Paulo S. de P. Herrmann[1] and Matheus Santos Lucas[2]

[1] Embrapa Instrumentation (CNPDIA), [2] Institute of Mathematics and Computer Sciences, University of São Paulo
São Carlos, SP, Brazil
e-mails: paulo.herrmann@embrapa.br, matsluccas@gmail.com

***Abstract*— Water stress significantly limits soybean (Glycine max L.) productivity worldwide. Early water stress detection is crucial for implementing timely irrigation strategies to mitigate its adverse effects. Electronic noses (E-Noses), equipped with sensor arrays that detect Volatile Organic Compounds (VOCs) emitted by plants, offer a non-invasive approach to monitoring plant health. This study proposes using radar chart areas as a novel method to evaluate the sensitivity of e-nose sensors in detecting water stress in soybeans. By converting multivariate sensor responses into radar charts, we quantitatively assess sensor performance and identify the most responsive sensors to water stress-induced VOC changes. The results demonstrate that radar chart areas provide a comprehensive metric for sensor sensitivity, enhancing the effectiveness of E-Noses in agricultural applications.**

Keywords- Radar charts; Electronic nose; Soybean; Water stress; Sensor sensitivity; Volatile Organic Compounds; Plant monitoring; Precision agriculture.

I. INTRODUCTION

Recent advances have introduced electronic noses (e-noses) as innovative tools for monitoring plant health. E-Noses consists of sensor arrays that can detect specific patterns of Volatile Organic Compounds (VOCs) emitted by plants under stress conditions (see Figure 1). Changes in VOC profiles can serve as early indicators of water stress, often appearing before any visual symptoms become noticeable [1].

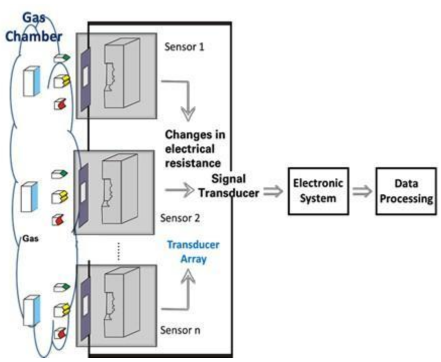

Figure 1. Block diagram of an E-nose and its components, including sensors, signal transducer, electronic system, and data processing.

Soybean (*Glycine max L.*) is a vital crop, serving as a key source of protein and oil for human consumption and animal feed. Water stress remains one of the most critical abiotic stresses affecting soybean growth and yield, leading to global economic losses. Traditional methods for detecting water stress involve physiological measurements and visual assessments, which can be labor-intensive and subjective.

The E-Nose has undergone extensive evaluation in experiments that employ statistical techniques such as Principal Component Analysis (PCA) and Linear Discriminant Analysis (LDA) to reduce the dimensionality of the collected data [2]. The dynamic mode is a distinguished method used to identify the most informative features for distinguishing between varying stress levels. A radar chart has been utilized for this purpose [1].

The radar chart, also known as a spider plot, star plot, or Kiviat figure [3], is more than just a graphical technique; it is a crucial tool in this study. It provides a straightforward way to display multivariate data on a two-dimensional plane, making it easier to visualize and compare sensor responses and ultimately evaluate the sensitivity of the sensors [1].

A radar chart presents multivariate data on axes that radiate outward from a central point. In Figure 2, each axis represents a distinct variable, with data points marked along these axes. Connecting these points forms a polygon, and calculating the area of this polygon can yield quantitative insights [4].

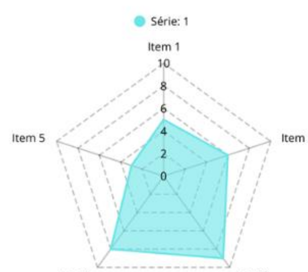

Figure 2. Radar Chart with an Area.

 ISBN: 978-1-68558-273-9

Takenaka et al. [5] provided a method for evaluating the accessibility of a facility location using the area of a radar chart. The authors argue that the area of a radar chart is a more stable measure of accessibility than other measures. The main objectives of this investigation are: 1. To develop a method utilizing radar chart areas to evaluate the sensitivity of E-Nose sensors in detecting water stress in soybean plants; 2. To identify which sensors within the E-Nose array are most responsive to VOC changes associated with water stress; 3. To assess the effectiveness of radar chart areas as a quantitative metric for sensor performance in agricultural monitoring applications.

The rest of the paper is structured as follows. In Section II, we present the materials and methods. In Section III, we show the results and discuss them. Conclusion and future work directives close the article, in Section IV.

II. MATERIALS AND METHODS

Below are presented all the materials and methods used in this work, as well as the equations used to obtain the results.

A. Plant Material and Experimental Design

Soybean seeds (*Glycine max L.*) were germinated and grown in controlled greenhouse conditions at 25.0±2.0 (°C), relative humidity of 60–70 (%), and a 14-hour photoperiod. Plants were cultivated in pots containing a standardized soil mixture and watered regularly to maintain optimal moisture levels.

Measurements were taken up to the V3 phenological stage of plant development. During the experiment (21 days), the plants were divided into two groups:

- Irrigated (10 days): Continued to receive regular irrigation to maintain field capacity.
- Non-irrigated (11 days): Subjected to water deficit by withholding irrigation to reduce soil moisture content gradually.

B. Electronic Nose Setup

An electronic nose system, AlphaFox^{tm} 2000, equipped with an array of six Complementary Metal-Oxide Semiconductor (CMOS) sensors was employed. Table 1 shows each sensor in the array was selected for its sensitivity to specific VOCs known to be emitted by plants under stress:

TABLE I. THE SENSORS INSTALLED IN THE E-NOSE ARE [6].

No.	Sensor	Sensitivity property	Reference Materials
S1	T30/1	Organic compounds	Organic compounds
S2	P10/1	Combustible gas	hydrocarbon
S3	P10/2	Inflammable gas	methane
S4	P40/1	Oxidizing gas	fluorine
S5	T70/2	Aromatic compounds	Methyl benzene, xylene
S6	PA/2	Organic compounds and toxic gas	Ammonia, amines, ethyl alcohol

C. Applications in Electronic Nose

The sensitivity S (%) for each sensor was calculated using (1):

$$S(\%) = \left(\frac{R - R_0}{R_0}\right) x100 \qquad (\%) \qquad (1)$$

R_0 – Initial electrical resistance (Ω);
R – Electrical resistance varying over time (Ω)

To analyze the data obtained from the E-Nose, we utilized both radar charts and area radar charts to represent the peak sensitivity (S (%)), which was normalized using Equation 1 for each of the six sensors: S1 T30/1, S2 P10/1, S3 P10/2, S4 P40/1, S5 T70/2, and S6 PA/2, as shown in Figure 3.

An area radar chart is a specific type of radar chart that illustrates the values by displaying the area enclosed by the lines connecting the data points. Figure 4 presents the representation of both the radar chart and the area radar chart for the peak sensitivity (S (%)). Radar charts are useful for visualizing multiple variables simultaneously [7].

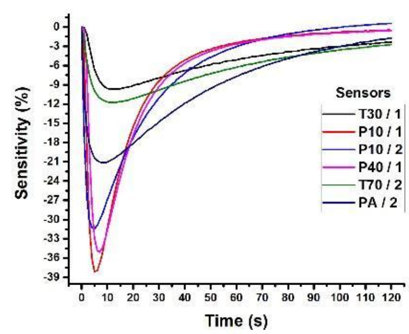

Figure 3. The variation in sensitivity, using the equation 1, of each of the six sensors in relation to time, depending on the gas sampled and measured in the E-Nose.

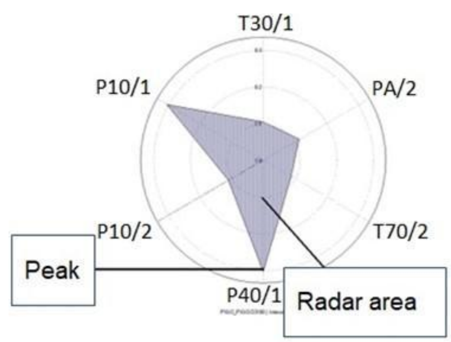

Figure 4. The radar chart and radar area from the sensitivity (%) peak to the six sensors (S1: T30/1; S2: P10/1; S3: P10/2; S4: P40/1; S5: T70/2 and S6: PA/2) from the E-Nose.

D. Calculating the Area of a Radar Chart

A radar chart is a graphical representation that effectively illustrates multidimensional data by expressing the values of each attribute in a clear and concise manner.

Its 2D visualization provides a comprehensive view of the data, making it easier to analyze and understand its various dimensions [8].

The method of radar chart for Multidimensional Data: X = {X1, X2Xj, ··· Xn} is a multi-dimensional data set, and Xi {xi1, xi2, xi3xiN} is a N-dimensional vector. Use the radar chart when N⩾3 [8].

A method for evaluating the accessibility of a facility location using the area of a radar chart was provided by Takenaka et al [5]. The authors argue that the area of a radar chart is a more stable measure of accessibility than other measures.

The Area of the Radar (An) was calculated using (2) where Xi = Si {S1(%), S2(%), S3(%), S4(%), S5(%), S6(%)}.

To calculate the area (A_n) of the polygon formed in a radar chart:

1. Convert Polar Coordinates to Cartesian Coordinates. Each data point is defined by:

- r_i: The distance from the center to the data point along axis i (the normalized value of the variable).
- θ_i: The angle corresponding to axis i, calculated as:

$$\theta_i = \frac{2\pi(i-1)}{n} \qquad (2)$$

Where n is the total number of variables (axes). The Cartesian coordinates (x_i,y_i) are:

$$x_i = r_i \cos\theta \text{ and } {}_i y_i = r_i \sin\theta_i$$

2. Apply the Shoelace Formula: The area of the polygon can be calculated using the Shoelace Formula (3):

$$A_n = \frac{1}{2}\left|\sum_{i=1}^{n}(x_i y_{i+1} - x_{i+1} y_i)\right| \quad (\%^2) \quad (3)$$

- $x_{n+1} = x_1$ and $y_{n+1} = y_1$ to complete the loop.

The formula sums the cross-products of vertex coordinates in a specific order [1].

III. RESULTS AND DISCUSSION

The average values and standard deviations derived from radar measurements of both irrigated and non-irrigated soybean samples are illustrated in Figure 5. The data reveals a marked difference between the measurements taken in the morning and those taken in the afternoon, with the greatest standard deviation observed during the afternoon sessions. This pronounced variation may be attributed to several influencing factors, including the physiological state of the plants, which can change due to water uptake and nutrient availability.

Environmental conditions at the time of sample extraction also likely played a significant role; the fluctuating temperatures, humidity levels, and light intensity throughout the day can affect the plants responses. Furthermore, the specific growth stage of the soybeans whether they are in vegetative growth or nearing maturation—can impact how they interact with their environment. Additionally, potential errors in the syringe headspace during sampling could introduce variability in the measurements.

It is particularly noteworthy that the highest standard deviation was recorded during the afternoon. On the 22nd day of the experiment, specific weather conditions were present, characterized by overcast skies, intermittent rain, and a significant cloud cover. These factors could have influenced the plants' physiological responses, leading to the observed discrepancies in the data.

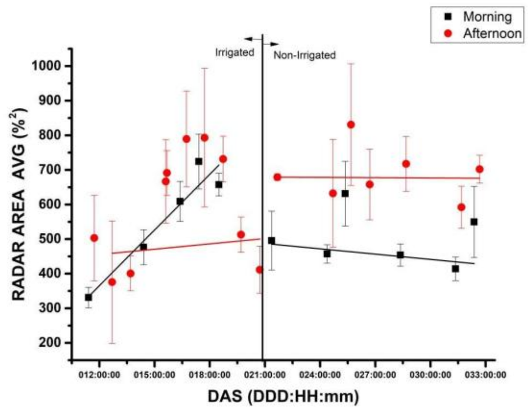

Figure 5. E-Nose measurements of gas samples taken from a chamber containing soybeans during the Days After Sowing (DAS), using the average radar area and standard deviation (n=3). The measurements are presented based on the time of day, either in the morning (9:30 a.m.) denoted by red circles or in the afternoon (3:30 p.m.) denoted by black squares. Moreover, the measurements are obtained from both irrigated and non-irrigated plants. For each DAS, gas samples are measured three times in both periods, i.e., the morning and afternoon to obtain the area radar measurement.

IV. CONCLUSIONS AND FUTURE WORK

An area radar chart is a specialized variant of a radar chart that utilizes the area enclosed by the connecting lines of data points to visually represent and compare values. Figure 4 illustrates this radar chart format, specifically highlighting the radar area at the sensitivity peak (S (%)), which indicates the maximum responsiveness of the variables in question.

Area radar charts are particularly valuable tools when analyzing and comparing the overall performance of distinct data groups, for example some experimental conditions. By presenting complex data in a clear and intuitive manner, area radar charts facilitate better decision-making and insights, allowing stakeholders to quickly grasp relationships and trends within the data. The area can be used as a valid metric to rank data.

Future work directions include integrating the method with equipment in a mobile unit to facilitate field use; integrating AI into the model; and applying the methodology to study thermal and water stress.

Acknowledgment

Embrapa Instrumentation supported this work and Embrapa project # 20.22.01.001.00.

References

[1] P. S. P. Herrmann, M. Santos Luccas, E. J. Ferreira and A. Torre Neto, "Application of electronic nose and machine learning used to detect soybean gases under water stress and variability throughout the daytime," *Front. Plant Sci.* 15:1323296, 2024, doi: 10.3389/fpls.2024.1323296.

[2] S. Zorpeykar, E. Mirzaee-Ghaleh, H. Karami, Z. Ramedani and A. D. Wilson, "Electronic Nose Analysis and Statistical Methods for Investigating Volatile Organic Compounds and Yield of Mint Essential Oils Obtained by Hydrodistillation," *Chemosensors*. vol. 10, no. 11, pp. 486+, 2022, https://doi.org/10.3390/chemosensors10110486.

[3] K. W. Kolence and P. J. Kiviat, "Software unit profiles & Kiviat figures," *ACM Sigmetrics. Performance Evaluation Review*, vol. 2, no. 3, pp. 2-12, 1973, doi: 10.1145/1041613.1041614.

[4] M. J. Saary, "Radar plots: a useful way for presenting multivariate health care data," *Journal of Clinical Epidemiology*, vol. 61, no. 4, pp. 311-317, 2008, https://doi.org/10.1016/j.jclinepi.2007.04.021.

[5] T. Takenaka, K. Nakamura, T. Ukai and Y. Ohsawa, "Stability of the Area of Radar Chart to Evaluate the Accessibility of Facility Location," *Journal of the City Planning Institute of Japan,* 2018.

[6] W. Wei, J. Li and L. Huang, "Discrimination of Producing Areas of Astragalus membranaceus Using Electronic Nose and UHPLC-PDA Combined with Chemometrics," *Czech J. Food Sci.*, vol. 35, no. 1, pp. 40-47, 2017, 10.17221/126/2016-CJFS.

[7] W - Y. Liu, B.-W. Wang, Jia-Xin Yu, Fang Li, Shui-Xing Wang and Wen-Xue Hong, "Visualization classification method of multi-dimensional data based on radar chart mapping," *2008 International Conference on Machine Learning and Cybernetics*, Kunming, China, pp. 857-862, 2008, doi: 10.1109/ICMLC.2008.4620524.

[8] W. Peng, "Improved radar chart for lighting system scheme selection," *Appl. Opt.*, vol. 61, no. 19, pp. 5619-5625, 2022, doi.org/10.1364/AO.455779.

ISBN: 978-1-68558-273-9